Wind and Structures, *Vol. 25, No. 2 (2017) 131-156*
DOI: https://doi.org/10.12989/was.2017.25.2.131

Dynamic stability of FG-CNT-reinforced viscoelastic micro cylindrical shells resting on nonhomogeneous orthotropic viscoelastic medium subjected to harmonic temperature distribution and 2D magnetic field

H. Tohidi[1], S.H. Hosseini-Hashemi[*1,2], A. Maghsoudpour[1] and S. Etemadi[1]

[1]*Department of Mechanical and Aerospace Engineering, Science and Research Branch, Islamic Azad University, Tehran, Iran*
[2]*School of mechanical Engineering Iran university of Science and Technology, Narmak, 16842-13114 Tehran, Iran*

(Received December 8, 2016, Revised April 20, 2017, Accepted July 19, 2017)

Abstract. This paper deals with the dynamic stability of embedded functionally graded (FG)-carbon nanotubes (CNTs)-reinforced micro cylindrical shells. The structure is subjected to harmonic non-uniform temperature distribution and 2D magnetic field. The CNT reinforcement is either uniformly distributed or FG along the thickness direction where the effective properties of nano-composite structure are estimated through Mixture low. The viscoelastic properties of structure are captured based on the Kelvin–Voigt theory. The surrounding viscoelastic medium is considered nonhomogeneous with the spring, orthotropic shear and damper constants. The material properties of cylindrical shell and the viscoelastic medium constants are assumed temperature-dependent. The first order shear deformation theory (FSDT) or Mindlin theory in conjunction with Hamilton's principle is utilized for deriving the motion equations where the size effects are considered based on Eringen's nonlocal theory. Based on differential quadrature (DQ) and Bolotin methods, the dynamic instability region (DIR) of structure is obtained for different boundary conditions. The effects of different parameters such as volume percent and distribution type of CNTs, mode number, viscoelastic medium type, temperature, boundary conditions, magnetic field, nonlocal parameter and structural damping constant are shown on the DIR of system. Numerical results indicate that the FGX distribution of CNTs is better than other considered cases. In addition, considering structural damping of system reduces the resonance frequency.

Keywords: dynamic stability; FG-CNT-reinforced visco-cylindrical shell; DQ and Bolotin methods; harmonic temperature distribution; 2D magnetic field

1. Introduction

Recently the subject of CNTs has attracted attentions of researchers because of their extraordinary physical and chemical properties such as high tensile strengths, high stiffness, high aspect ratio and low density (Iijima 1991, Yakobson *et al.* 1996, Saito *et al.* 1998). A large number

*Corresponding author, Dr., E-mail: shh@iust.ac.ir

http://www.techno-press.org/?journal=was&subpage=8 ISSN: 1226-6116 (Print), 1598-6225 (Online)

of investigations are carried out to study different aspect of behavior of CNTs and the results of these studies shows that CNTs have excellent mechanical, electronic, electromechanical and thermal properties (Yu *et al*. 2000, Pan *et al*. 2001). Due to the remarkable properties, it has also been used as reinforcement for nanocomposites that may significantly improve the mechanical, electrical and thermal properties of the resulting nanocomposites; However, the majority of CNT-reinforced composite study has been focused on the polymer matrix composites (Qian *et al*. 2002, Wan *et al*. 2005, Esawi and Farag 2007, Li and Wang 2008, Zamanian *et al*. 2017). A great deal of interest for the analysis of carbon nanotube-reinforced composite (CNTRC) structures is being manifested in the specialized literature. This interest is mainly due to the advent of the new composite material systems exhibiting exotic properties as compared to the traditional, carbon fiber-reinforced composite structures. Due to their very attractive thermo-mechanical properties these new materials are going to play a great role in the construction of Micro-Electro Mechanical Systems (MEMS) and Nano-Electro-Mechanical Systems (NEMS) (Liew *et al*. 2015, Koizumi 1993, Anon 1996).

Since shells among the fundamental engineering structures have many industrial applications. Extensive research has been done in different field of shell behavior consisting free vibration (Paliwal 1996), forced vibration (Rogacheva 1998), mechanical and thermal buckling (Bich *et al*. 2013, Alijani *et al*. 2015). Loy *et al*. (1999) considered the vibration of functionally graded cylindrical shells. They showed that the natural frequency of functionally graded cylindrical shell will increase in comparison with isotropic. Pradhan (2000) presented Rayleigh method is used to derive the governing equation of Vibration characteristics of functionally graded cylindrical shells under various boundary conditions. Mechanism of ovalling vibrations of cylindrical shells in cross flow was presented by Tsujiguchi and Yamada (2001). A geometrically nonlinear wind-induced vibration analysis strategy for large-span single-layer reticulated shell structures based on the nonlinear finite element method was introduced by Li and Tamura (2005). Haddadpour *et al*. (2007) studied the free vibration analysis of functionally graded cylindrical shells including thermal effects. The motion equations are obtained based on Love's shell theory and the von Karman–Donnell-type of kinematic nonlinearity and the Galerkin method is used to solving equations. Haddadpour *et al*. (2011) analyzed the vibration of functionally graded cylindrical shells with ring support. The governing equations of motion are obtained using an energy functional and by applying the Ritz. It is assumed that the Material properties are graded in the thickness direction, according to the power-law volume fraction function method. The influence of changes in shell geometrical parameters and variations of ring support position on vibration characteristics are considered. Khalili (2012) analyzed the free vibration analysis of homogeneous isotropic circular cylindrical shells based on a new three-dimensional refined higher-order theory. The equations of motion are derived using Hamilton's principle. Solutions are obtained based on Galerkin method. The present theory gives more accurate results in contrast to the other theories. Zhou (2012) considered the free vibrations of cylindrical shells with elastic-support boundary conditions. According to the Flügge classical thin shell theory, the motion equations of cylindrical shells are solved by using the wave propagations method. Jin *et al*. (2013) studied an exact solution for the free vibration analysis of composite cylindrical shells with general elastic boundary conditions. Xuyuan *et al*. (2015) investigated the vibration analyses of symmetrically laminated composite cylindrical shells with arbitrary boundaries conditions via Rayleigh-Ritz method. They have analyzed the effect of boundary rigidity and lamination on natural frequency behavior. Hosseini-Hashemi *et al*. (2015) implemented the free vibrations of functionally graded viscoelastic cylindrical panel under various boundary conditions. The materials are assumed to be functionally

graded viscoelastic (FGV). Results are compared for various boundary conditions, thickness to radius ratios and shallowness angles. Jin *et al.* (2016) described a unified solution for the vibration analysis of functionally graded material (FGM) doubly-curved shells of revolution with arbitrary boundary conditions. The solution was derived by means of the modified Fourier series method (Ye and Jin 2016, Ye *et al*. 2016). Three-dimensional (3D) vibration analysis of FG sandwich deep open shells with general boundary restraints, including open spherical shells and the cylindrical ones was presented by Ye *et al*. (2016).

Shen *et al*. (2012) investigated the nonlinear vibration of nanotube-reinforced composite cylindrical shells in thermal environments. Two types of CNT-reinforced composite (CNTRC) shells, namely, uniformly distributed (UD) and FG reinforcements, are available. The material properties of FG-CNTRC shells are assumed to be varied in the thickness direction. They used higher-order shear deformation theory for deriving equations of motion. The results show that in most cases the natural frequencies of FG-CNTRC shell with symmetrical distribution of CNTs are higher. Alibeigloo *et al*. (2013) used nonlocal theory to investigate the vibration of CNTs. The state equations obtained from constitutive relations and governing motion equations are solved analytically by applying of the state space method. They showed that by considering the nonlocal parameter causes the CNTs more flexible and reduces the natural frequencies. Also natural frequency of SWCNTs clearly is impressed by both axial and circumferential wave numbers. Alibeigloo (2014) analyzed the free vibration analysis of functionally graded CNT reinforced composite cylindrical panel embedded in piezoelectric layers by using theory of elasticity. By using state space technique across the thickness direction, state space differential equations are solved analytically. The analysis was carried out by using the Fourier series expansion across the axial and circumferential directions. The results suggest that dimensionless frequency of CNTRC cylindrical panel in the case of FG, at a same point are always greater in comparison with corresponding points in the other cases of CNT distribution. Song *et al*. (2015) studied the Vibration analysis of CNT-reinforced functionally graded composite cylindrical shells in thermal environments. They have used Reddy's high-order shear deformation theory for structural modeling. The equations of motion are obtained based on FSDT and TSDT. The results are validated with high-order shear deformation theory. They showed that the CNTs can increase the stiffness of the whole structure. They used numerical method to calculate the free vibration responses. Civalek *et al*. (2016) studied free vibration of carbon nanotubes reinforced (CNTR) and functionally graded shells and plates based on FSDT via discrete singular convolution method. The equations are based on First order shear deformation and five types of distributions of CNTR material are also considered. Mirzaei *et al*. (2016) presented the free vibration of FG-CNT-reinforced composite cylindrical panels. To establish the eigenvalue problem of the system, the energy based Ritz method with Chebyshev polynomials as the basis functions is implemented. The results show frequencies of the panel are dependent to both, volume fraction of CNTs and their distribution pattern across the thickness. By increasing the volume fraction of CNTs, the frequencies of the panel increases.

According to the best authors of knowledge, no report has been found in the literature on the dynamic stability analysis of FG-CNT-reinforced micro cylindrical shell subjected to harmonic non-uniform temperate distribution and 2D magnetic field. In the present study, the orthotropic Mindlin plate theory is used for nonlinear bending behavior of polymeric temperature-dependent plates reinforced by SWCNTs resting on orthotropic temperature-dependent elastomeric medium. For CNTRC plate, both cases of uniform and FG distribution patterns of SWCNT reinforcements are considered. The equivalent material properties of nano-composite structure are obtained based

on the rule of mixture. Considering the size and structural damping effects, the nonlinear motion equations are obtained based on Hamilton's principal along with the Mindlin theory. DQM and Bolotin methods are utilized for calculating the DIR of FG-CNT-reinforced cylindrical shell. The main issues of this paper is considering the effects of the volume percent and distribution type of CNTs, viscoelastic medium type, temperature, boundary conditions, mode number, magnetic field, nonlocal parameter and structural damping constant on the dynamic stability bahaviour of the structure.

2. Basic relations

2.1 Mixture rule

For obtaining the equivalent material properties of two-phase nano-composites (i.e., polymer as matrix and CNT as reinforcer), the mixture rule is utilized. Based on the mixture rule, the effective Young and shear moduli of FG-CNT-reinforced cylindrical shell can be written as (Shen and Xiang 2012)

$$E_{11} = \eta_1 V_{CNT} E_{r11} + (1 - V_{CNT}) E_m, \tag{1}$$

$$\frac{\eta_2}{E_{22}} = \frac{V_{CNT}}{E_{r22}} + \frac{(1 - V_{CNT})}{E_m}, \tag{2}$$

$$\frac{\eta_3}{G_{12}} = \frac{V_{CNT}}{G_{r12}} + \frac{(1 - V_{CNT})}{G_m}, \tag{3}$$

where E_{r11}, E_{r22} and G_{r11} indicate the Young's moduli and shear modulus of CNTs, respectively; and E_m, G_m represent the corresponding properties of the isotropic matrix; η_j (j= 1, 2, 3) shows the scale-dependent material properties; V_{CNT} and V_m are the volume fractions of the CNTs and matrix, respectively. The uniform and three types of FG distributions of the CNTs along the thickness direction of the structure take the following forms

$$UD: \quad V_{CNT} = V_{CNT}^*, \tag{4}$$

$$FGV: \quad V_{CNT}(z) = \left(1 - \frac{2z}{h}\right) V_{CNT}^*, \tag{5}$$

$$FGO: \quad V_{CNT}(z) = 2\left(1 - \frac{2|z|}{h}\right) V_{CNT}^*, \tag{6}$$

$$FGX: \quad V_{CNT}(z) = 2\left(\frac{2|z|}{h}\right) V_{CNT}^*, \tag{7}$$

where

$$V_{CNT}^{*}=\frac{w_{CNT}}{w_{CNT}+\left(\rho_{CNT}/\rho_{m}\right)-\left(\rho_{CNT}/\rho_{m}\right)w_{CNT}}, \tag{8}$$

where w_{CNT}, ρ_m and ρ_{CNT} are the mass fraction of the CNT, the densities of the matrix and CNT, respectively. Similarly, the thermal expansion coefficients in the longitudinal and transverse directions respectively (α_{11} and α_{22}) and the density (ρ) of the CNT-reinforced cylindrical shell can be determined as

$$\rho=V_{CNT}^{*}\rho_{r}+V_{m,}\rho_{m,}, \tag{9}$$

$$\alpha_{11}=V_{CNT}^{*}\alpha_{r11}+V_{m,}\alpha_{m,}, \tag{10}$$

$$\alpha_{22}=\left(1+\nu_{r12}\right)V_{CNT}\alpha_{r22}+\left(1+\nu_{m}\right)V_{m}\alpha_{m}-\nu_{12}\alpha_{11}, \tag{11}$$

where α_{r11}, α_{r22} and α_m are the thermal expansion coefficients of the CNT and matrix, respectively. It should be noted that ν_{12} is assumed as constant over the thickness of the structure.

2.2 Visco-nonlocal theory

Based on the Eringen's nonlocal elasticity theory, the stress state at a reference point in the body is regarded to be dependent not only on the strain state at this point but also on the strain states at all of the points throughout the body. The relation between stress (σ_{ij}) and strain (ε_{ij}) in nonlocal form may be expressed as (Eringen 1972)

$$\left(1-\left(e_0a\right)^2\nabla^2\right)\begin{Bmatrix}\sigma_{xx}\\ \sigma_{\theta\theta}\\ \sigma_{\theta z}\\ \sigma_{zx}\\ \sigma_{x\theta}\end{Bmatrix}=\begin{bmatrix}C_{11}(z,T) & C_{12}(z,T) & 0 & 0 & 0\\ C_{21}(z,T) & C_{22}(z,T) & 0 & 0 & 0\\ 0 & 0 & C_{44}(z,T) & 0 & 0\\ 0 & 0 & 0 & C_{55}(z,T) & 0\\ 0 & 0 & 0 & 0 & C_{66}(z,T)\end{bmatrix}\begin{Bmatrix}\varepsilon_{xx}-\alpha_{xx}\Delta T\\ \varepsilon_{\theta\theta}-\alpha_{\theta\theta}\Delta T\\ \gamma_{\theta z}\\ \gamma_{xz}\\ \gamma_{x\theta}\end{Bmatrix}, \tag{12}$$

where e_0a is the small scale parameter, ∇^2 is the Laplace operator; C_{ij} and $\alpha_{xx},\alpha_{\theta\theta}$ denote the temperature-dependent elastic coefficients are the thermal expansion constants, respectively which can be obtained using rule of mixture (section 2.1). Noted that the temperature distribution across the thickness direction follows a harmonic law as follows (Fazzolari 2015, Madani *et al*. 2016)

$$T(\mathrm{z})=\Delta T\left(1-\cos\left[\frac{\pi}{2}\left(\frac{z}{h}+\frac{1}{2}\right)\right]\right)+T_i, \qquad \Delta T=T_o-T_i. \tag{13}$$

where T_o and T_i are the outer and inner surfaces temprature, repectively.

With respect to this fact that all materials exhibit viscoelastic response, however, according to

Kelvin–Voigt (Kolahchi *et al*. 2016a) at real life, C_{ij} depend on the time variation as follows

$$C_{ij} = C_{ij}\left(1 + g\frac{\partial}{\partial t}\right), \tag{14}$$

where g is the structural damping constant.

2.3 FSDT or Mindlin theory

In the classical shell theory, the cross-section rotations and the shear strains in *z* direction are neglected. These shortcomings are fixed in the FSDT. According to the assumption of FSDT cylindrical shell theory, the displacement field can be written as (Reddy 2002)

$$u(x,\theta,z,t) = u(x,\theta,t) + z\phi_x(x,\theta,t), \tag{15}$$

$$v(x,\theta,z,t) = v(x,\theta,t) + z\phi_\theta(x,\theta,t), \tag{16}$$

$$w(x,\theta,z,t) = w(x,\theta,t), \tag{17}$$

where $(u(x,\theta,z,t), v(x,\theta,z,t), w(x,\theta,z,t))$ denote the displacement components at an arbitrary point (x,θ,z) in the cylindrical shell, $(u(x,\theta,t), v(x,\theta,t), w(x,\theta,t))$ are the displacement of a material point at (x,θ) on the mid-plane (i.e., $z=0$) of the shell along the *x*-, θ-, and *z*-directions, respectively; ϕ_x and ϕ_θ are the rotations of the normal to the mid-plane about x- and θ- directions, respectively. Based on above relations, the nonlinear strain-displacement equations may be written as

$$\varepsilon_{xx} = \frac{\partial u}{\partial x} + z\frac{\partial \phi_x}{\partial x} + \frac{1}{2}\left(\frac{\partial w}{\partial x}\right)^2, \tag{18}$$

$$\varepsilon_{\theta\theta} = \frac{1}{R}\left(w + \frac{\partial v}{\partial \theta}\right) + \frac{z}{R}\frac{\partial \phi_\theta}{\partial \theta} + \frac{1}{2}\left(\frac{\partial w}{R\partial \theta}\right)^2, \tag{19}$$

$$\gamma_{x\theta} = \frac{\partial v}{\partial x} + \frac{1}{R}\left(\frac{\partial u}{\partial \theta}\right) + z\left(\frac{\partial \phi_\theta}{\partial x} + \frac{1}{R}\frac{\partial \phi_x}{\partial \theta}\right) + \frac{\partial w}{\partial x}\frac{\partial w}{R\partial \theta}, \tag{20}$$

$$\gamma_{xz} = \phi_x + \frac{\partial w}{\partial x}, \tag{21}$$

$$\gamma_{z\theta} = \frac{1}{R}\left(\frac{\partial w}{\partial \theta} - v\right) + \phi_\theta. \tag{22}$$

where $(\varepsilon_{xx}, \varepsilon_{\theta\theta})$ are the normal strain components and $(\gamma_{\theta z}, \gamma_{xz}, \gamma_{x\theta})$ are the shear strain components.

3. Motion equations

The schematic figure of an embedded FG-CNT-reinforced micro-visco cylindrical shell with length L, radius R and thickness h is shown in Fig. 1. The structure is subjected to harmin axial load and the surrounding medium is modeled with spring, orthotropic shear and damper constants. For obtaining the motion equations of presented structure, the energy method and Hamilton's principal are applied.

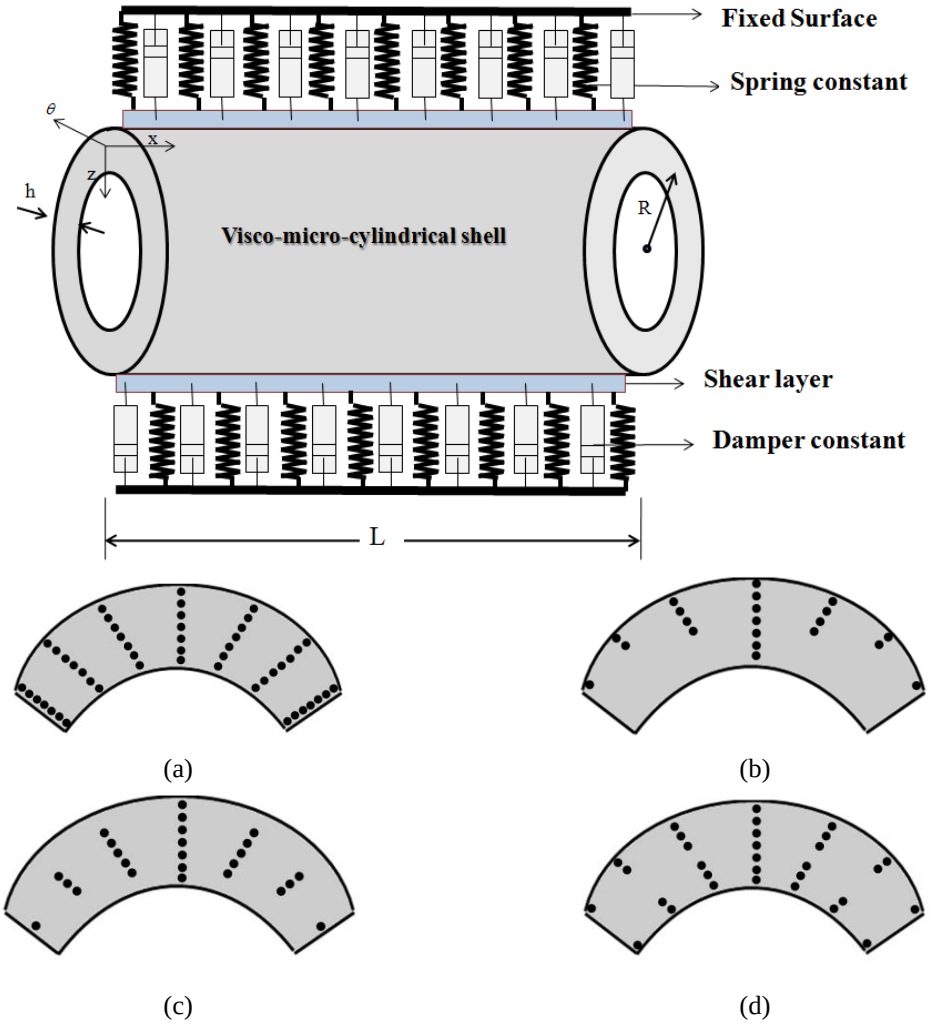

Fig. 1 A schematic figure for embedded FG-CNT-reinforced viscoelastic micro cylindrical shell subjected to harmonic temperature distribution and magnetic field

3.1 Potential energy

The total potential energy of nano-composite cylindrical shell can be expressed as

$$U = \frac{1}{2}\int \left(\sigma_{xx}\varepsilon_{xx} + \sigma_{\theta\theta}\varepsilon_{\theta\theta} + \sigma_{xz}\varepsilon_{xz} + \sigma_{\theta z}\varepsilon_{\theta z} + \sigma_{x\theta}\gamma_{x\theta}\right)dV \,. \tag{23}$$

Substituting strain-displacement relations from Eqs. (18)-(22), the above equation may be expanded as

$$\begin{aligned} U = \frac{1}{2}\int_0^{2\pi}\int_0^L \Bigg\{ & N_{xx}\left(\frac{\partial u}{\partial x} + \frac{1}{2}\left(\frac{\partial w}{\partial x}\right)^2\right) + M_{xx}\frac{\partial \phi_x}{\partial x} + \frac{N_{\theta\theta}}{R}\left(w + \frac{\partial v}{\partial \theta} + \frac{1}{2}\left(\frac{\partial w}{R\partial \theta}\right)^2\right) \\ & + \frac{M_{\theta\theta}}{R}\frac{\partial \phi_\theta}{\partial \theta} + Q_x\left(\phi_x + \frac{\partial w}{\partial x}\right) + N_{x\theta}\left[\frac{\partial v}{\partial x} + \frac{1}{R}\frac{\partial u}{\partial \theta} + \frac{\partial w}{\partial x}\frac{\partial w}{R\partial \theta}\right] \\ & + M_{x\theta}\left[\frac{\partial \phi_\theta}{\partial x} + \frac{1}{R}\frac{\partial \phi_x}{\partial \theta}\right] + Q_\theta\left[\frac{1}{R}\left(\frac{\partial w}{\partial \theta} - v\right) + \phi_\theta\right]\Bigg\} R\,dx\,d\theta \end{aligned} \tag{24}$$

where the stress resultant-displacement relations can be written as

$$\begin{Bmatrix} N_{xx} \\ N_{\theta\theta} \\ N_{x\theta} \end{Bmatrix} = \int_{-\frac{h}{2}}^{\frac{h}{2}} \begin{Bmatrix} \sigma_{xx} \\ \sigma_{\theta\theta} \\ \tau_{x\theta} \end{Bmatrix} dz \tag{25}$$

$$\begin{Bmatrix} Q_x \\ Q_\theta \end{Bmatrix} = k' \int_{-\frac{h}{2}}^{\frac{h}{2}} \begin{Bmatrix} \sigma_{xz} \\ \sigma_{\theta z} \end{Bmatrix} dz \tag{26}$$

$$\begin{Bmatrix} M_{xx} \\ M_{\theta\theta} \\ M_{x\theta} \end{Bmatrix} = \int_{-\frac{h}{2}}^{\frac{h}{2}} \begin{Bmatrix} \sigma_{xx} \\ \sigma_{\theta\theta} \\ \tau_{x\theta} \end{Bmatrix} z\,dz \tag{27}$$

In which k' is shear correction coefficient. Substituting Eqs. (12) and (18)-(22) into Eqs. (25)-(27), the stress resultant-displacement relations can be expressed as

$$N_{xx} = A_{110}\left(\frac{\partial u}{\partial x} + \frac{1}{2}\left(\frac{\partial w}{\partial x}\right)^2\right) + A_{111}\frac{\partial \phi_x}{\partial x} + A_{120}\left(\frac{\partial v}{R\partial \theta} + \frac{w}{R} + \frac{1}{2}\left(\frac{\partial w}{R\partial \theta}\right)^2\right) + A_{121}\frac{\partial \phi_\theta}{R\partial \theta}, \tag{28}$$

$$N_{\theta\theta} = A_{120}\left(\frac{\partial u}{\partial x} + \frac{1}{2}\left(\frac{\partial w}{\partial x}\right)^2\right) + A_{121}\frac{\partial \phi_x}{\partial x} + A_{220}\left(\frac{\partial v}{R\partial \theta} + \frac{w}{R} + \frac{1}{2}\left(\frac{\partial w}{R\partial \theta}\right)^2\right) + A_{221}\frac{\partial \phi_\theta}{R\partial \theta}, \tag{29}$$

$$Q_\theta = k^{'} A_{44}\left[\frac{1}{R}\left(\frac{\partial w}{\partial \theta} - v\right) + \phi_\theta\right], \tag{30}$$

$$Q_x = k^{'} A_{55}\left(\frac{\partial w}{\partial x} + \phi_x\right), \tag{31}$$

$$N_{x\theta} = A_{660}\left(\frac{\partial u}{R\partial\theta} + \frac{\partial v}{\partial x} + \frac{\partial w}{\partial x}\frac{\partial w}{R\partial\theta}\right) + A_{661}\left(\frac{\partial \phi_x}{R\partial\theta} + \frac{\partial \phi_\theta}{\partial x}\right), \tag{32}$$

$$M_{xx} = A_{111}\frac{\partial u}{\partial x} + A_{112}\frac{\partial \phi_x}{\partial x} + A_{121}\left(\frac{\partial v}{R\partial\theta} + \frac{w}{R}\right) + A_{122}\frac{\partial \phi_\theta}{R\partial\theta}, \tag{33}$$

$$M_{\theta\theta} = A_{121}\frac{\partial u}{\partial x} + A_{122}\frac{\partial \phi_x}{\partial x} + A_{221}\left(\frac{\partial v}{R\partial\theta} + \frac{w}{R}\right) + A_{222}\frac{\partial \phi_\theta}{R\partial\theta}, \tag{34}$$

$$M_{x\theta} = A_{661}\left(\frac{\partial u}{R\partial\theta} + \frac{\partial v}{\partial x}\right) + A_{662}\left(\frac{\partial \phi_x}{R\partial\theta} + \frac{\partial \phi_\theta}{\partial x}\right), \tag{35}$$

where

$$A_{ijk} = \int_{-h/2}^{h/2} C_{ij} z^{k} dz, \qquad k = 0,1,2,\ i,j = 1,2,6 \tag{36}$$

$$A_{ii} = \int_{-h/2}^{h/2} C_{ii} dz, \quad \mathrm{i} = 4,5 \tag{37}$$

3.2 Kinetic energy

The kinetic energy of nano-composite structure can be expressed as follows

$$K = \frac{\rho}{2}\int\left(\left(\frac{\partial u}{\partial t} + z\frac{\partial \phi_x}{\partial t}\right)^2 + \left(\frac{\partial v}{\partial t} + z\frac{\partial \phi_\theta}{\partial t}\right)^2 + \left(\frac{\partial w}{\partial t}\right)^2\right)dV. \tag{38}$$

Simplifying the above relation, we have

$$K = \frac{1}{2}\int\begin{pmatrix} I_0\left(\left(\frac{\partial u}{\partial t}\right)^2 + \left(\frac{\partial v}{\partial t}\right)^2 + \left(\frac{\partial w}{\partial t}\right)^2\right) + I_1\left(2\frac{\partial u}{\partial t}\frac{\partial \phi_x}{\partial t} + 2\frac{\partial v}{\partial t}\frac{\partial \phi_\theta}{\partial t}\right) \\ + I_2\left(\left(\frac{\partial \phi_x}{\partial t}\right)^2 + \left(\frac{\partial \phi_\theta}{\partial t}\right)^2\right)\end{pmatrix} dA, \tag{39}$$

where the moments of inertia can be defined as

$$\begin{Bmatrix} I_0 \\ I_1 \\ I_2 \end{Bmatrix} = \int_{z^{(k-1)}}^{z^{(k)}} \begin{bmatrix} \rho \\ \rho z \\ \rho z^2 \end{bmatrix} dz, \tag{40}$$

3.3 External works

External works in this paper are due to the nonhomogeneous viscoelastic medium and 2D magnetic field.

3.3.1 Nonhomogeneous viscoelastic medium

The external work due to the nonhomogeneous viscoelastic medium can be expressed as (Kolahchi *et al.* 2016a, Mosharrafian and Kolahchi 2016)

$$W_e = \int_0^{2\pi}\int_0^{L} \begin{pmatrix} -k_w w - C_d \dot{w} + G_\xi \left(\cos^2\theta w_{,xx} + 2\cos\theta\sin\theta w_{,yx} + \sin^2\theta w_{,yy}\right) \\ + G_\eta \left(\sin^2\theta w_{,xx} - 2\sin\theta\cos\theta w_{,yx} + \cos^2\theta w_{,yy}\right) \end{pmatrix} dA, \tag{41}$$

where θ describes the local ξ direction of orthotropic foundation with respect to the global x-axis of the shell; G_ξ and G_η are the shear constants in ξ and η directions, respectively; C_d is the damper constant; k_w is the spring constant which may be written as a nonhomogeneous form as follows (Mosharrafian and Kolahchi 2016)

$$k_W = k_0\left(1 - \beta\exp\left(-\alpha x^2\right)\right), \tag{42}$$

where $\alpha > 1, 0 < \beta < 1$. The foundation stiffness k_0 for soft medium may be written by

$$K_w = \frac{\dfrac{E_s}{\left(1-\nu_s^2\right)}}{4L\left[1-\left(\dfrac{\nu_s}{(1-\nu_s)}\right)^2\right](2-c_1)^2}\left[5-\left(2\gamma_1^2+6\gamma_1+5\right)\exp\left(-2\gamma_1\right)\right], \tag{43}$$

where

$$c_1 = \left(\frac{H_s}{L}+2\right)\exp\left(-\frac{H_s}{L}\right), \tag{44}$$

where E_s, ν_s, H_s are Young's modulus, Poisson's ratio and depth of the foundation, respectively. In this paper, E_s is assumed to be temperature-dependent while ν_s is assumed to be a constant.

3.3.2 2D magnetic field

Due to existence of CNTs as reinforcer in the shell, the structure is sensitive to magnetic field. The exerted body force due to the magnetic field, $\mathbf{H_0}$ can be written as (Kolahchi *et al*. 2016b)

$$\mathbf{f}_m = \underbrace{\eta\left(\nabla\times\underbrace{\left(\nabla\times\left(\mathbf{u}\times\mathbf{H}_0\right)\right)}_{\mathbf{h}}\right)}_{\mathbf{J}}\times\mathbf{H}_0, \tag{45}$$

where η is the magnetic permeability of the CNTs; ∇ is the gradient operator; $\mathbf{u}=(u,v,w)$ is the displacement field vector; $\mathbf{h}$ is the disturbing vectors of magnetic field; $\mathbf{J}$ is the current density and $\mathbf{H_0}$ for the unidirectional state can be defined as $\mathbf{H_0}=H_x\delta_{x\vartheta}\hat{e}_x+H_\theta\delta_{\theta\vartheta}\hat{e}_\theta$ where δ is the Kronecker delta tensor. Using Eqs. (1)-(3), the Lorentz force per unit volume can be expressed as

$$f_x=\eta H_\theta^2\delta_{\theta\vartheta}\left[\left(\frac{\partial^2 u}{\partial x^2}+\frac{\partial^2 u}{R^2\partial\theta^2}\right)+z\left(\frac{\partial^2\phi_x}{\partial x^2}+\frac{\partial^2\phi_x}{R^2\partial\theta^2}\right)\right], \tag{46}$$

$$f_\theta=\eta H_x^2\delta_{x\vartheta}\left[\left(\frac{\partial^2 v}{\partial x^2}+\frac{\partial^2 v}{R^2\partial\theta^2}\right)+z\left(\frac{\partial^2\phi_\theta}{R^2\partial\theta^2}+\frac{\partial^2\phi_\theta}{\partial x^2}\right)\right], \tag{47}$$

$$f_z=\eta\left[H_\theta^2\delta_{\theta\vartheta}\left(\frac{\partial^2 w}{\partial x^2}+\frac{\partial\phi_\theta}{R\partial\theta}\right)+H_x^2\delta_{x\vartheta}\left(\frac{\partial^2 w}{\partial x^2}+\frac{\partial\phi_\theta}{R\partial\theta}\right)\right]. \tag{48}$$

The resultant Lorentz's forces and the corresponding bending moments may be expressed as

$$\left(F_x^m,F_\theta^m,F_z^m\right)=\int_{-h/2}^{h/2}\left(f_x,f_\theta,f_z\right)dz, \tag{49}$$

$$\left(M_x^m,M_\theta^m,M_z^m\right)=\int_{-h/2}^{h/2}\left(f_x,f_\theta,f_z\right)zdz, \tag{50}$$

Substituting Eqs. (46)-(48) into Eqs. (49) and (50) yields

$$F_x^m=\eta h H_\theta^2\delta_{\theta\vartheta}\left(\frac{\partial^2 u}{\partial x^2}+\frac{\partial^2 u}{R^2\partial\theta^2}\right), \tag{51}$$

$$F_\theta^m=\eta h H_x^2\delta_{x\vartheta}\left(\frac{\partial^2 v}{\partial x^2}+\frac{\partial^2 v}{R^2\partial\theta^2}\right), \tag{52}$$

$$F_z^m=\eta h\left[H_\theta^2\delta_{\theta\vartheta}\left(\frac{\partial^2 w}{\partial x^2}+\frac{\partial\varphi_\theta}{R\partial\theta}\right)+H_x^2\delta_{x\vartheta}\left(\frac{\partial^2 w}{\partial x^2}+\frac{\partial\varphi_\theta}{R\partial\theta}\right)\right], \tag{53}$$

$$M_x^m = \frac{\eta h^3 H_\theta^2}{12}\delta_{\theta\vartheta}\left(\frac{\partial^2\phi_x}{\partial x^2}+\frac{\partial^2\phi_x}{R^2\partial\theta^2}\right), \tag{54}$$

$$M_\theta^m = \frac{\eta h^3 H_x^2}{12}\delta_{x\vartheta}\left(\frac{\partial^2\phi_\theta}{R^2\partial\theta^2}+\frac{\partial^2\phi_\theta}{\partial x^2}\right). \tag{55}$$

3.4 Hamilton's principal

The Hamilton's principal can be written as follows

$$\int_0^t(\delta U-\delta K-\delta W)dt=0. \tag{56}$$

Substituting Eqs. (24), (39), (41) and (51)-(55) into Eq. (56) yields the following motion equations

$$\delta u:\frac{\partial N_{xx}}{\partial x}+\frac{\partial N_{x\theta}}{R\partial\theta}+F_x^m=I_0\frac{\partial^2 u}{\partial t^2}+I_1\frac{\partial^2\varphi_x}{\partial t^2}, \tag{57}$$

$$\delta v:\frac{\partial N_{x\theta}}{\partial x}+\frac{\partial N_{\theta\theta}}{R\partial\theta}+\frac{Q_\theta}{R}+F_\theta^m=I_0\frac{\partial^2 v}{\partial t^2}+I_1\frac{\partial^2\varphi_\theta}{\partial t^2}, \tag{58}$$

$$\begin{aligned}\delta w:&\frac{\partial Q_x}{\partial x}+\frac{\partial Q_\theta}{R\partial\theta}-\frac{N_{\theta\theta}}{R}+N_{xx}\frac{\partial^2 w}{\partial x^2}+N_{\theta\theta}\frac{\partial^2 w}{R^2\partial\theta^2}\\&-k_w w-C_d\dot{w}+G_\xi\left(\cos^2\theta\frac{\partial^2 w}{\partial x^2}+2\cos\theta\sin\theta\frac{\partial^2 w}{R\partial x\partial\theta}+\sin^2\theta\frac{\partial^2 w}{R^2\partial\theta^2}\right)\\&+G_\eta\left(\sin^2\theta\frac{\partial^2 w}{\partial x^2}-2\sin\theta\cos\theta\frac{\partial^2 w}{R\partial x\partial\theta}+\cos^2\theta\frac{\partial^2 w}{R^2\partial\theta^2}\right)+F_z^m=I_0\frac{\partial^2 w}{\partial t^2},\end{aligned} \tag{59}$$

$$\delta\phi_x:\frac{\partial M_{xx}}{\partial x}+\frac{\partial M_{x\theta}}{R\partial\theta}-Q_x+M_x^m=I_2\frac{\partial^2\phi_x}{\partial t^2}+I_1\frac{\partial^2 u}{\partial t^2}, \tag{60}$$

$$\delta\phi_\theta:\frac{\partial M_{x\theta}}{\partial x}+\frac{\partial M_{\theta\theta}}{R\partial\theta}-Q_\theta+M_\theta^m=I_2\frac{\partial^2\phi_\theta}{\partial t^2}+I_1\frac{\partial^2 v}{\partial t^2}, \tag{61}$$

Substituting Eqs. (28) to (35) into Eqs. (57) to (61), the motion equations can be expanded as

$$\begin{aligned}&A_{110}\left(\frac{\partial^2 u}{\partial x^2}+\frac{\partial w}{\partial x}\frac{\partial^2 w}{\partial x^2}\right)+A_{111}\frac{\partial^2\phi_x}{\partial x^2}+A_{120}\left(\frac{\partial^2 v}{R\partial x\partial\theta}+\frac{\partial w}{R^2\partial x}+\frac{\partial w}{R\partial\theta}\frac{\partial^2 w}{R\partial x\partial\theta}\right)+A_{121}\frac{\partial^2\phi_\theta}{R\partial\theta\partial x}\\&+A_{660}\left(\frac{\partial^2 u}{R^2\partial\theta^2}+\frac{\partial^2 v}{R\partial x\partial\theta}+\frac{\partial w}{R\partial\theta}\frac{\partial^2 w}{R\partial x\partial\theta}+\frac{\partial w}{\partial x}\frac{\partial^2 w}{R^2\partial\theta^2}\right)+A_{661}\left(\frac{\partial^2\phi_\theta}{R\partial x\partial\theta}+\frac{\partial^2\phi_x}{R^2\partial\theta^2}\right)\\&+g\frac{\partial}{\partial t}\left[A_{110}\left(\frac{\partial^2 u}{\partial x^2}+\frac{\partial w}{\partial x}\frac{\partial^2 w}{\partial x^2}\right)+A_{111}\frac{\partial^2\phi_x}{\partial x^2}+A_{120}\left(\frac{\partial^2 v}{R\partial x\partial\theta}+\frac{\partial w}{R^2\partial x}+\frac{\partial w}{R\partial\theta}\frac{\partial^2 w}{R\partial x\partial\theta}\right)+A_{121}\frac{\partial^2\phi_\theta}{R\partial\theta\partial x}\right.\\&\left.+A_{660}\left(\frac{\partial^2 u}{R^2\partial\theta^2}+\frac{\partial^2 v}{R\partial x\partial\theta}+\frac{\partial w}{R\partial\theta}\frac{\partial^2 w}{R\partial x\partial\theta}+\frac{\partial w}{\partial x}\frac{\partial^2 w}{R^2\partial\theta^2}\right)+A_{661}\left(\frac{\partial^2\phi_\theta}{R\partial x\partial\theta}+\frac{\partial^2\phi_x}{R^2\partial\theta^2}\right)\right]\\&+\eta hH_\theta^2\delta_{\theta\vartheta}\left(\frac{\partial^2 u}{\partial x^2}+\frac{\partial^2 u}{R^2\partial\theta^2}\right)=I_0\frac{\partial^2 u}{\partial t^2}+I_1\frac{\partial^2\phi_x}{\partial t^2},\end{aligned} \tag{62}$$

$$A_{120}\left(\frac{\partial^2 u}{R\partial x\,\partial\theta}+\frac{\partial w}{\partial x}\frac{\partial^2 w}{R\partial x\,\partial\theta}\right)+A_{121}\frac{\partial^2\phi_x}{R\partial x\,\partial\theta}+A_{220}\left(\frac{\partial^2 v}{R^2\partial\theta^2}+\frac{\partial w}{R\partial\theta}\frac{\partial^2 w}{R^2\partial\theta^2}\right)$$
$$+A_{221}\frac{\partial^2\phi_\theta}{R^2\partial\theta^2}+A_{660}\left(\frac{\partial^2 v}{\partial x^2}+\frac{\partial^2 u}{R\partial x\,\partial\theta}+\frac{\partial w}{R\partial\theta}\frac{\partial^2 w}{\partial x^2}+\frac{\partial w}{\partial x}\frac{\partial^2 w}{R\partial x\,\partial\theta}\right)+A_{661}\left(\frac{\partial^2\phi_x}{R\partial\theta\partial x}+\frac{\partial^2\phi_\theta}{\partial x^2}\right)$$
$$+g\frac{\partial}{\partial t}\left[A_{120}\left(\frac{\partial^2 u}{R\partial x\,\partial\theta}+\frac{\partial w}{\partial x}\frac{\partial^2 w}{R\partial x\,\partial\theta}\right)+A_{121}\frac{\partial^2\phi_x}{R\partial x\,\partial\theta}+A_{220}\left(\frac{\partial^2 v}{R^2\partial\theta^2}+\frac{\partial w}{R\partial\theta}\frac{\partial^2 w}{R^2\partial\theta^2}\right)\right.$$
$$\left.+A_{221}\frac{\partial^2\phi_\theta}{R^2\partial\theta^2}+A_{660}\left(\frac{\partial^2 v}{\partial x^2}+\frac{\partial^2 u}{R\partial x\,\partial\theta}+\frac{\partial w}{R\partial\theta}\frac{\partial^2 w}{\partial x^2}+\frac{\partial w}{\partial x}\frac{\partial^2 w}{R\partial x\,\partial\theta}\right)+A_{661}\left(\frac{\partial^2\phi_x}{R\partial\theta\partial x}+\frac{\partial^2\phi_\theta}{\partial x^2}\right)\right]$$
$$+\eta h H_x^{2}\delta_{x\vartheta}\left(\frac{\partial^2 v}{\partial x^2}+\frac{\partial^2 v}{R^2\partial\theta^2}\right)=I_0\frac{\partial^2 v}{\partial t^2}+I_1\frac{\partial^2\phi_\theta}{\partial t^2},\tag{63}$$

$$k'A_{44}\left[\frac{1}{R^2}\left(\frac{\partial^2 w}{\partial\theta^2}-\frac{\partial v}{\partial\theta}\right)+\frac{1}{R}\frac{\partial\phi_\theta}{\partial\theta}\right]+k'A_{55}\left(\frac{\partial^2 w}{\partial x^2}+\frac{\partial\phi_x}{\partial x}\right)$$
$$-A_{120}\frac{\partial u}{\partial x}-A_{121}\frac{\partial\phi_x}{\partial x}-A_{220}\left(\frac{\partial v}{R^2\partial\theta}+\frac{w}{R^2}+\frac{1}{2R}\left(\frac{\partial w}{R\partial\theta}\right)^2\right)-A_{221}\frac{\partial\phi_\theta}{R\partial\theta}$$
$$+g\frac{\partial}{\partial t}\left[k'A_{44}\left[\frac{1}{R^2}\left(\frac{\partial^2 w}{\partial\theta^2}-\frac{\partial v}{\partial\theta}\right)+\frac{1}{R}\frac{\partial\phi_\theta}{\partial\theta}\right]+k'A_{55}\left(\frac{\partial^2 w}{\partial x^2}+\frac{\partial\phi_x}{\partial x}\right)\right.$$
$$\left.-A_{120}\frac{\partial u}{\partial x}-A_{121}\frac{\partial\phi_x}{\partial x}-A_{220}\left(\frac{\partial v}{R^2\partial\theta}+\frac{w}{R^2}+\frac{1}{2R}\left(\frac{\partial w}{R\partial\theta}\right)^2\right)-A_{221}\frac{\partial\phi_\theta}{R\partial\theta}\right]$$
$$+N_{xx}^{f}\frac{\partial^2 w}{\partial x^2}+N_{\theta\theta}^{f}\frac{\partial^2 w}{R^2\partial\theta^2}-k_w w-C_d\dot{w}$$
$$+G_\xi\left(\cos^2\theta\frac{\partial^2 w}{\partial x^2}+2\cos\theta\sin\theta\frac{\partial^2 w}{R\partial x\,\partial\theta}+\sin^2\theta\frac{\partial^2 w}{R^2\partial\theta^2}\right)$$
$$+G_\eta\left(\sin^2\theta\frac{\partial^2 w}{\partial x^2}-2\sin\theta\cos\theta\frac{\partial^2 w}{R\partial x\,\partial\theta}+\cos^2\theta\frac{\partial^2 w}{R^2\partial\theta^2}\right)$$
$$+\eta h\left[H_\theta^{2}\delta_{\theta\vartheta}\left(\frac{\partial^2 w}{\partial x^2}+\frac{\partial\varphi_\theta}{R\partial\theta}\right)+H_x^{2}\delta_{x\vartheta}\left(\frac{\partial^2 w}{\partial x^2}+\frac{\partial\varphi_\theta}{R\partial\theta}\right)\right]=I_0\frac{\partial^2 w}{\partial t^2},\tag{64}$$

$$A_{111}\frac{\partial^2 u}{\partial x^2}+A_{112}\frac{\partial^2\phi_x}{\partial x^2}+A_{121}\left(\frac{\partial^2 v}{R\partial\theta\partial x}+\frac{1}{R}\frac{\partial w}{\partial x}\right)+A_{122}\frac{\partial^2\phi_\theta}{R^2\partial\theta^2}+$$
$$A_{661}\left(\frac{\partial^2 u}{R^2\partial\theta^2}+\frac{\partial^2 v}{R\partial x\,\partial\theta}\right)+A_{662}\left(\frac{\partial^2\phi_x}{R^2\partial\theta^2}+\frac{\partial^2\phi_\theta}{R\partial x\,\partial\theta}\right)-k'A_{55}\left(\frac{\partial w}{\partial x}+\phi_x\right)$$
$$+g\frac{\partial}{\partial t}\left[A_{111}\frac{\partial^2 u}{\partial x^2}+A_{112}\frac{\partial^2\phi_x}{\partial x^2}+A_{121}\left(\frac{\partial^2 v}{R\partial\theta\partial x}+\frac{1}{R}\frac{\partial w}{\partial x}\right)+A_{122}\frac{\partial^2\phi_\theta}{R^2\partial\theta^2}+\right.$$
$$\left.A_{661}\left(\frac{\partial^2 u}{R^2\partial\theta^2}+\frac{\partial^2 v}{R\partial x\,\partial\theta}\right)+A_{662}\left(\frac{\partial^2\phi_x}{R^2\partial\theta^2}+\frac{\partial^2\phi_\theta}{R\partial x\,\partial\theta}\right)-k'A_{55}\left(\frac{\partial w}{\partial x}+\phi_x\right)\right]$$
$$+\frac{\eta h^3 H_\theta^{2}}{12}\delta_{\theta\vartheta}\left(\frac{\partial^2\varphi_x}{\partial x^2}+\frac{\partial^2\varphi_x}{R^2\partial\theta^2}\right)=I_2\frac{\partial^2\phi_x}{\partial t^2}+I_1\frac{\partial^2 u}{\partial t^2},\tag{65}$$

$$A_{121}\frac{\partial^2 u}{R\partial x\partial\theta}+A_{122}\frac{\partial^2\phi_x}{R\partial x\partial\theta}+A_{221}\left(\frac{\partial^2 v}{R^2\partial\theta^2}+\frac{1}{R^2}\frac{\partial w}{\partial\theta}\right)+A_{222}\frac{\partial^2\phi_\theta}{R^2\partial\theta^2}$$
$$+A_{661}\left(\frac{\partial^2 u}{R\partial\theta\partial x}+\frac{\partial^2 v}{\partial x^2}\right)+A_{662}\left(\frac{\partial^2\phi_x}{R\partial\theta\partial x}+\frac{\partial^2\phi_\theta}{\partial x^2}\right)-k'A_{44}\left[\frac{1}{R}\left(\frac{\partial w}{\partial\theta}-v\right)+\phi_\theta\right]$$
$$+g\frac{\partial}{\partial t}\left[A_{121}\frac{\partial^2 u}{R\partial x\partial\theta}+A_{122}\frac{\partial^2\phi_x}{R\partial x\partial\theta}+A_{221}\left(\frac{\partial^2 v}{R^2\partial\theta^2}+\frac{1}{R^2}\frac{\partial w}{\partial\theta}\right)+A_{222}\frac{\partial^2\phi_\theta}{R^2\partial\theta^2}\right.$$
$$\left.+A_{661}\left(\frac{\partial^2 u}{R\partial\theta\partial x}+\frac{\partial^2 v}{\partial x^2}\right)+A_{662}\left(\frac{\partial^2\phi_x}{R\partial\theta\partial x}+\frac{\partial^2\phi_\theta}{\partial x^2}\right)-k'A_{44}\left[\frac{1}{R}\left(\frac{\partial w}{\partial\theta}-v\right)+\phi_\theta\right]\right]$$
$$+\frac{\eta h^3 H_x^2}{12}\delta_{x,\vartheta}\left(\frac{\partial^2\varphi_\theta}{R^2\partial\theta^2}+\frac{\partial^2\varphi_\theta}{\partial x^2}\right)=I_2\frac{\partial^2\phi_\theta}{\partial t^2}+I_1\frac{\partial^2 v}{\partial t^2},\tag{66}$$

In this paper, three types of boundary conditions are considered as follows

- **Simple-Simple (SS)**

$$x=0,L\Rightarrow u=v=w=\phi_\theta=M_x=0,\tag{67}$$

- **Clamped- Clamped (CC)**

$$x=0,L\Rightarrow u=v=w=\phi_x=\phi_\theta=0,\tag{68}$$

- **Clamped- Simple (CS)**

$$x=0\Rightarrow u=v=w=\phi_x=\phi_\theta=0,$$
$$x=L\Rightarrow u=v=w=\phi_\theta=M_x=0.\tag{69}$$

4. Solution procedure

4.1 DQ method

In the DQ method, the differential equations can be changed into a first order algebraic equation by employing appropriate weighting coefficients. In other words, the partial derivatives of a function are approximated with respect to *x* and θ as follows (Kolahchi *et al*. 2016a, b)

$$\frac{d^n f_x(x_i,\theta_j)}{dx^n}=\sum_{k=1}^{N_x}A_{ik}^{(n)}f(x_k,\theta_j)\qquad n=1,...,N_x-1,\tag{70}$$

$$\frac{d^m f_y(x_i,\theta_j)}{d\theta^m}=\sum_{l=1}^{N_\theta}B_{jl}^{(m)}f(x_i,\theta_l)\qquad m=1,...,N_\theta-1,\tag{71}$$

$$\frac{d^{n+m} f_{xy}(x_i,\theta_j)}{dx^n d\theta^m}=\sum_{k=1}^{N_x}\sum_{l=1}^{N_\theta}A_{ik}^{(n)}B_{jl}^{(m)}f(x_k,\theta_l),\tag{72}$$

A more superior choice for the positions of the grid points is Chebyshev polynomials as expressed

$$x_i = \frac{L}{2}\left[1-\cos\left(\frac{i-1}{N_x-1}\right)\pi\right] \qquad i=1,...,N_x \tag{73}$$

$$\theta_i = \frac{2\pi}{2}\left[1-\cos\left(\frac{i-1}{N_\theta-1}\right)\pi\right] \qquad i=1,...,N_\theta \tag{74}$$

also $A_{ik}^{(n)}$ and $B_{jl}^{(m)}$ are the weighting coefficients associated with n[th]-order partial derivative of $F(x,\theta)$ with respect to x at the discrete point x_i and m[th]-order derivative with respect to θ at θ_i, respectively which may be calculated as

$$A_{ij}^{(1)} = \begin{cases} \dfrac{M(x_i)}{(x_i-x_j)M(x_j)} & for \quad i\neq j, \quad i,j=1,2,...,N_x \\ -\sum\limits_{\substack{j=1\\ i\neq j}}^{N_x} A_{ij}^{(1)} & for \quad i=j, \quad i,j=1,2,...,N_x \end{cases} \tag{75}$$

$$B_{ij}^{(1)} = \begin{cases} \dfrac{P(\theta_i)}{(\theta_i-\theta_j)P(\theta_j)} & for \quad i\neq j, \quad i,j=1,2,...,N_\theta, \\ -\sum\limits_{\substack{j=1\\ i\neq j}}^{N_\theta} B_{ij}^{(1)} & for \quad i=j, \quad i,j=1,2,...,N_\theta \end{cases} \tag{76}$$

where

$$M(x_i) = \prod_{\substack{j=1\\ j\neq i}}^{N_x}(x_i-x_j) \tag{77}$$

$$P(\theta_i) = \prod_{\substack{j=1\\ j\neq i}}^{N_\theta}(\theta_i-\theta_j) \tag{78}$$

For higher order derivatives we have

$$A_{ij}^{(n)} = n\left(A_{ii}^{(n-1)}A_{ij}^{(1)} - \frac{A_{ij}^{(n-1)}}{(x_i-x_j)}\right) \tag{79}$$

$$B_{ij}^{(m)} = m\left(B_{ii}^{(m-1)} B_{ij}^{(1)} - \frac{B_{ij}^{(m-1)}}{(\theta_i - \theta_j)} \right) \tag{80}$$

The harmonic axial load P is considered as

$$P(t) = \beta P_{cr} + \alpha P_{cr} \cos(\omega t), \tag{81}$$

where ω is the frequency of excitation, P_{cr} is the static stability load, β and α may be defined as static and dynamic load factors, respectively. Finally, the motion equations coupled with boundary conditions in matrix form can be expressed as

$$\left\{ [K_L + K_{NL} - \beta P_{cr} K_G - \alpha P_{cr} \cos(\omega t) K_G] \begin{bmatrix} d_b \\ d_d \end{bmatrix} + [C_L + C_{NL}] \begin{bmatrix} \dot{d}_b \\ \dot{d}_d \end{bmatrix} + [M] \begin{bmatrix} \ddot{d}_b \\ \ddot{d}_d \end{bmatrix} \right\} = [0], \tag{82}$$

where $[d] = [u\ v\ w\ \phi_x\ \phi_\theta]^T$; $[KL]$ and $[KNL]$ are respectively, linear and nonlinear stiffness matrixes; $[KL]$ is the coefficient of force; $[C_L]$ and $[C_{NL}]$ are respectively, linear and nonlinear damp matrixes and $[M]$ is the mass matrix; the subscripts of *b* and *d* are related to boundary and domain points, respectively.

4.2 Bolotin method

In order to determinate the boundaries of dynamic instability regions, the method suggested by Bolotin (Kolahchi *et al.* 2016a) is applied. Hence, the components of $\{d\}$ can be written in the Fourier series with period $2T$ as

$$\{d\} = \sum_{k=1,3,\ldots}^{\infty} \left[\{a\}_k \sin\frac{k\omega t}{2} + \{b\}_k \cos\frac{k\omega t}{2} \right], \tag{83}$$

Substituting Eq. (83) into Eq. (82) and setting the coefficients of each sine and cosine as well as the sum of the constant terms to zero, yields

$$\left| \left([K_L + K_{NL}] - P_{cr}\alpha [K]_G \pm P_{cr} \frac{\beta}{2} [K]_G \mp [C]\frac{\omega}{2} - [M]\frac{\omega^2}{4} \right) \right| = 0, \tag{84}$$

Solving the above equation based on eigenvalue problem, the variation of ω with respect to α can be plotted as DIR.

5. Numerical results

In this section, the effects of different parameters on the dynamic stability of embedded visco-micro cylindrical shell are studied. For this purpose, the cylinder is made from Poly methyl

methacrylate (PMMA) with the constant Poisson's ratios of $\nu_m = 0.34$, temperature-dependent thermal coefficient of $\alpha_m = (1 + 0.0005\Delta T) \times 10^{-6} / K$, and temperature-dependent Young moduli of $E_m = (3.52 - 0.0034T) GPa$ in which $T = T_0 + \Delta T$ and $T_0 = 300\ K$ (room temperature). In addition, (10, 10) SWCNTs are selected as reinforcements with the material properties listed in Table 1. The elastomeric medium is made of Poly dimethylsiloxane (PDMS) which the temperature-dependent material properties of which are assumed to be $\nu_s = 0.48$ and $E_s = (3.22 - 0.0034T) GPa$ in which $T = T_0 + \Delta T$ and $T_0 = 300\ K$ (room temperature) (Shen and Xiang 2012, Kolahchi *et al*. 2016b).

5.1 DQ Convergence

The convergence and accuracy of the DQ method in calculating the excitation frequency and DIR of the nano-composite structure is shown in Fig. 2. It can be seen that with increasing the number of grid points, the DIR shifts to lower frequencies and in N=15, the results become converge. However, in the present work, the number of grid points for obtaining the accurate results is assumed 15.

Table 1 Temperature-dependent material properties of (10, 10) SWCNT (L= 9.26 nm, R= 0.68 nm, h= 0.067 nm, $\upsilon_{12}^{CNT} = 0.175$)

V_{CNT}	MD (Liew *et al*. 2014)		Rule of mixture			
	E_{11} (GPa)	E_{22} (GPa)	E_{11} (GPa)	η_1	E_{22} (GPa)	η_2
0.11	94.8	2.2	94.57	0.149	2.2	0.934
0.14	120.2	2.3	120.09	0.150	2.3	0.942
0.17	145.6	3.5	145.08	0.149	3.5	1.381

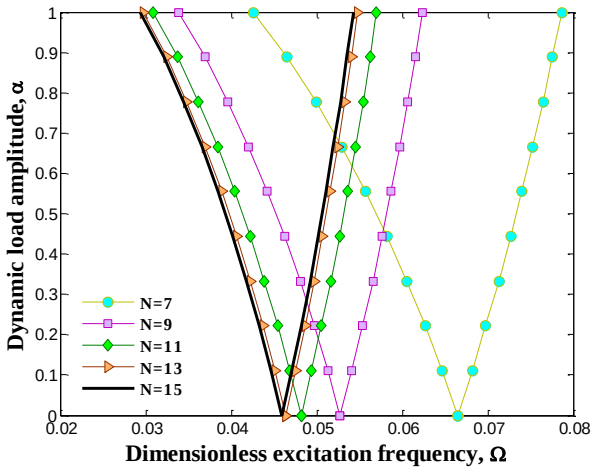

Fig. 2 The effect of DQ grid points number on the DIR of structure

5.2 Validation

In order to validate the results of this work, neglecting viscoelastic medium, 2D magnetic field, structural damping parameter, nonlocal effects and harmonic temperature distribution, present results are compared with those reported by Lei *et al*. (2014). For this purpose, a FGX-CNT-reinforced simply supported cylindrical shell with *R/h=200* is considered based on Love's thin shell theory. Using DQ and Bolotin methods, the dimensionless excitation frequency ($\Omega = \omega R\sqrt{\rho(1-\nu_{12}\nu_{21})/\mathrm{E}_{22}}$) with respect to the dynamic to static load factor (α/β) is plotted in Fig. 3 for the first four modes. As can be seen, present results obtained by DQM are in good agreement with those reported by Lei *et al*. (2014) based on the mesh-free kp-Ritz method, indicating validation of this work.

5.3 Effects of different parameters

Here, the effects of different parameters on the dimensionless excitation frequency ($\Omega = \omega R\sqrt{\rho(1-\nu_{12}\nu_{21})/\mathrm{E}_{22}}$) versus dynamic load factor (i.e., α) are shown in Figs. 4-10.

These figures indicate the DIR of structure where the regions inside and outside the boundary curves correspond to unstable (parametric resonance) and stable regions, respectively.

The effect of distribution type of CNT in visco-micro-cylindrical shell on the DIR is shown in Fig. 4 where the UD and three types of FG distribution patterns are considered. It can be found that the DIR of FGA- and FGO- CNT-reinforced visco-micro-cylindrical shell is lower than the DIR of UD ones while the FGX-CNT-reinforced visco-micro-cylindrical shell has higher DIR with respect to three other cases. It is because the stiffness of CNT-reinforced visco-micro-cylindrical changes with the form of CNT distribution in matrix. However, it can be concluded that CNT distribution close to top and bottom are more efficient than those distributed nearby the mid-plane for increasing the stiffness of cylindrical shell.

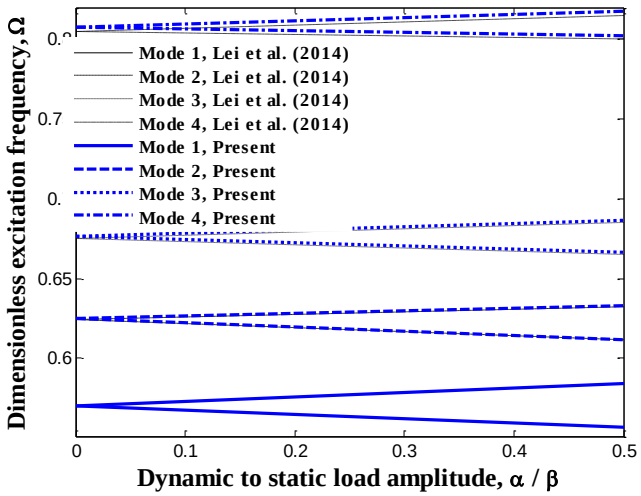

Fig. 3 Validation of this work with Lei *et al*. (2014)

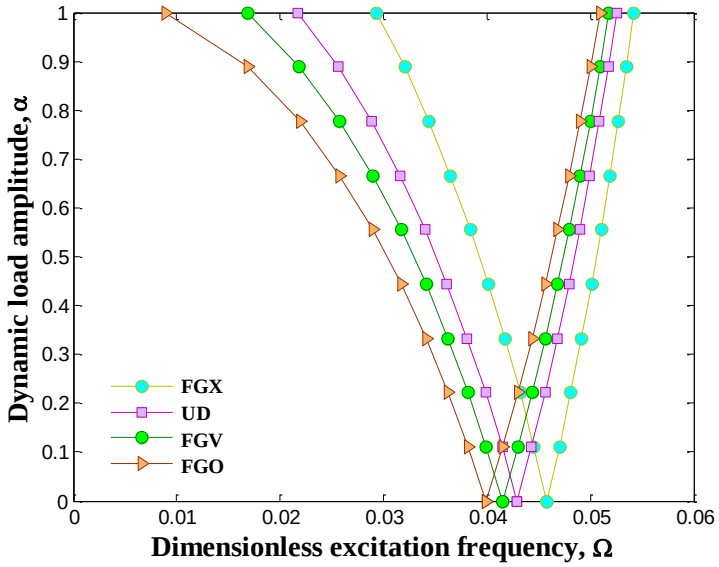

Fig. 4 The effect of CNT distribution on the DIR of structure

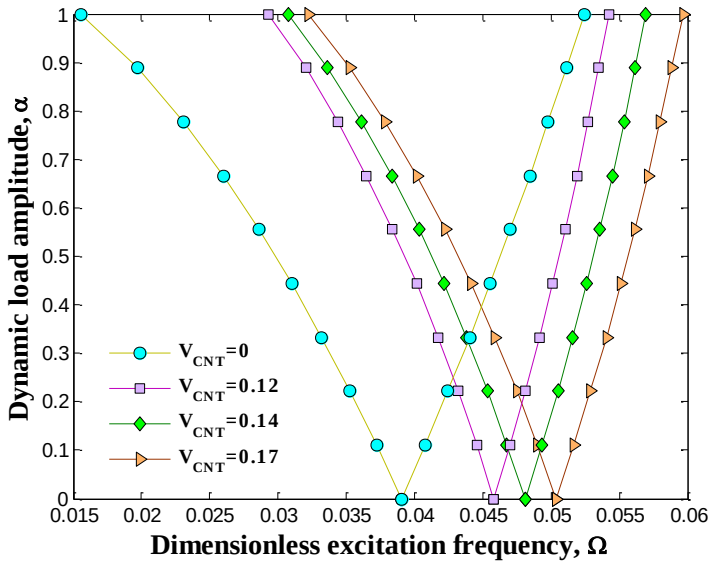

Fig. 5 The effect of CNT volume percent on the DIR of structure

Fig. 5 demonstrates the effect of the CNT volume fraction on the DIR of the structure. As can be seen with increasing the CNT volume fraction, the DIR shifts to higher excitation frequencies. It means that the resonance frequency increases with increasing the CNT volume fraction. Physically, with increasing the CNT volume fraction, the stiffness of structure increases.

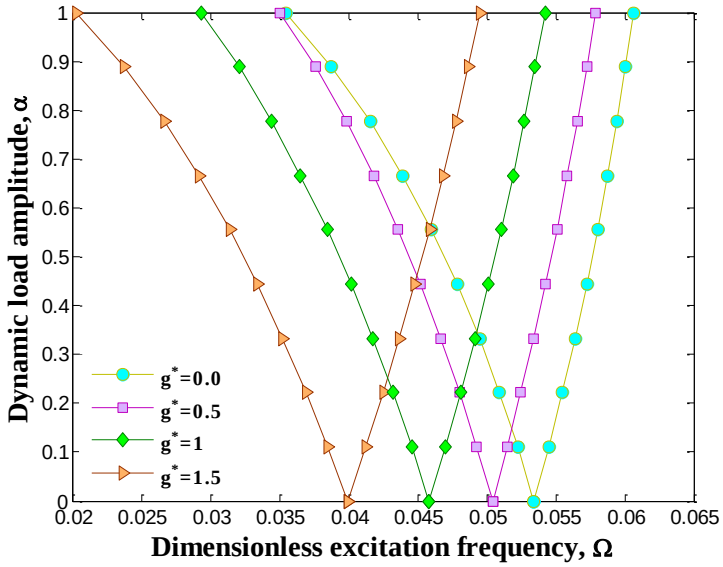

Fig. 6 The effect of structural damping on the DIR of structure

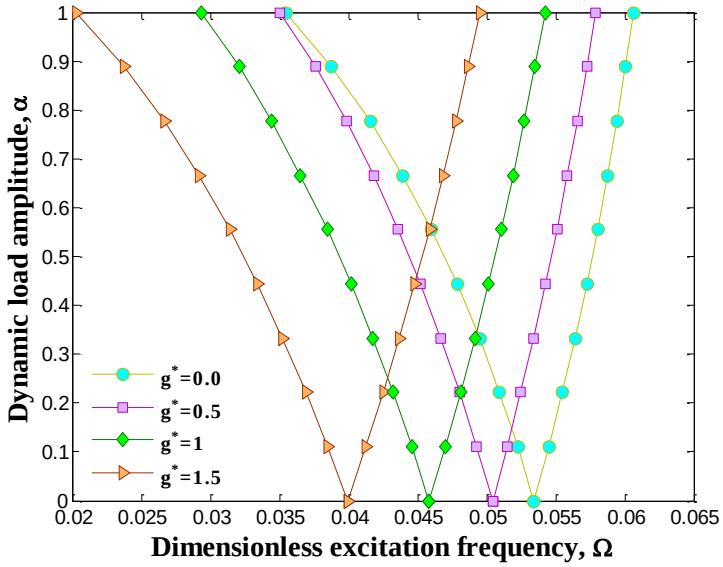

Fig. 7 The effect of nonlocal parameter on the DIR of structure

The dimensionless structural damping effects ($g^* = g / L^2\sqrt{E_{11}h^2/\rho}$) are demonstrated in Fig. 6 on the DIR of structure. It can be concluded that with increasing the structural damping parameter, the DIR happens in higher excitation frequencies. This remarkable difference shows

that considering the nature of structure as viscoelastic can yields the accurate results with respect to non-visco ones. The reason is that assuming viscoelastic structure means induce of damping force which results in more absorption of energy by the system.

In order to show the nonlocal parameter effects on the DIR of structure, Fig. 7 is plotted. It is obvious that considering size affects leads to higher excitation frequency. In other words, the DIR of system shifts to higher frequencies with assuming the nonlocal effects. It is due to the fact that nonlocal theory introduces a more flexible model wherein atoms are joined by elastic springs while the values of spring constants in local theory are supposed to be infinite.

The effect of the magnetic field on the DIR of the CNT-reinforced micro cylindrical shell is depicted in Fig. 8. As can be seen, the excitation frequency of structure increases with increasing magnetic field. It is due to the fact that with increasing the magnetic field, the stiffness of system is enhanced. However, the magnetic field is one of the main parameters for control of the resonance frequency of structure.

The DIR of the CNTR-reinforced visco-micro-cylindrical shell is presented in Fig. 9 for four cases of without medium (WM), nonhomogeneous visco-Winkler (NVW) medium, orthotropic nonhomogeneous visco-Pasternak (ONVP) medium and nonhomogeneous visco-Pasternak (NVP) medium. Obviously, considering every types of viscoelastic medium increases the excitation frequency of structure and shifts the DIR to right. It is due to the fact that considering viscoelastic medium leads to stiffer structure. Furthermore, the excitation frequency predicted by ONVP or NVP is higher than that predicated by NVW. It is because the NVW is capable to describe just normal load of while the ONVP or NVP describes both transverse shear and normal loads of the elastomeric medium. In addition, the DIR of NVP is happened in higher frequency with respect to ONVP since in ONVP, the shear layer is considered with the degree of 45 with respect to x axis.

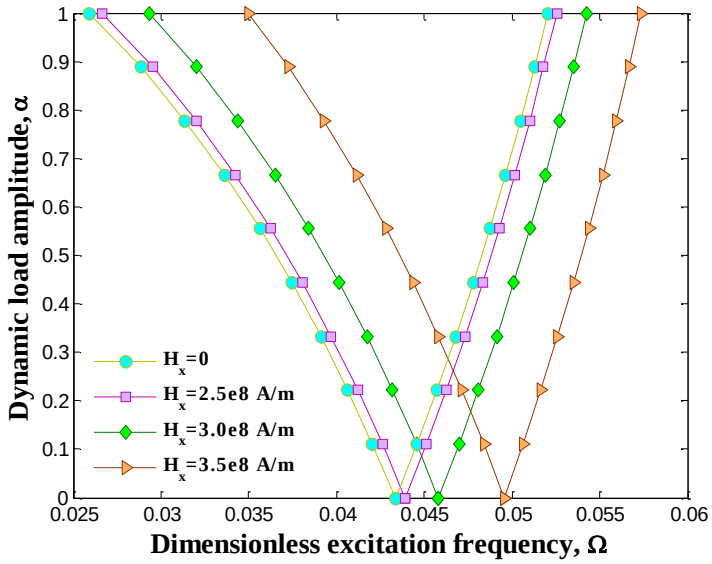

Fig. 8 The effect of viscoelastic medium type on the DIR of structure

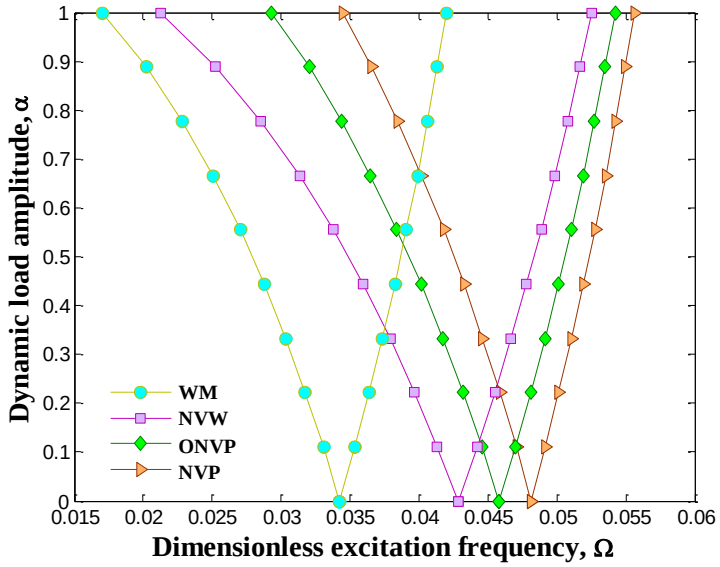

Fig. 9 The effect of boundary conditions on the DIR of structure

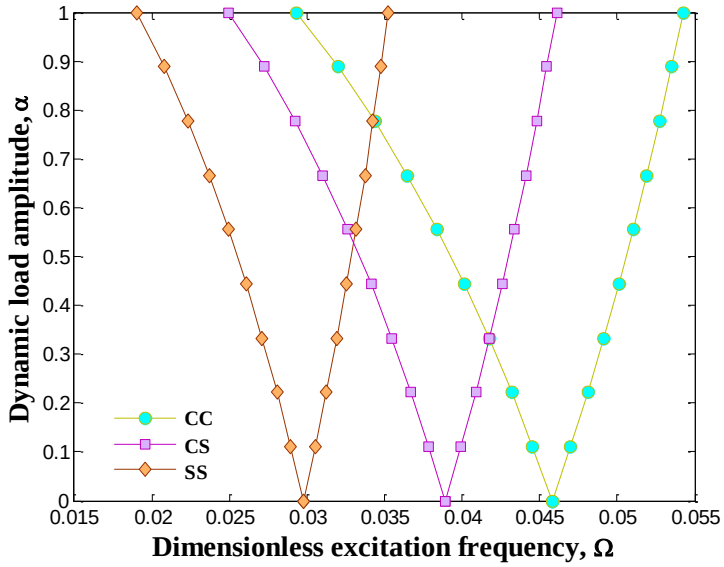

Fig. 10 The effect of boundary conditions on the DIR of structure

The effect of the different boundary condition on the DIR of structure is showed in Fig. 10. It can be found that the resonance frequency predicted by CC cylindrical shell is higher with respect to other considered boundary conditions. It is because that considering CC boundary condition leads to harder structure.

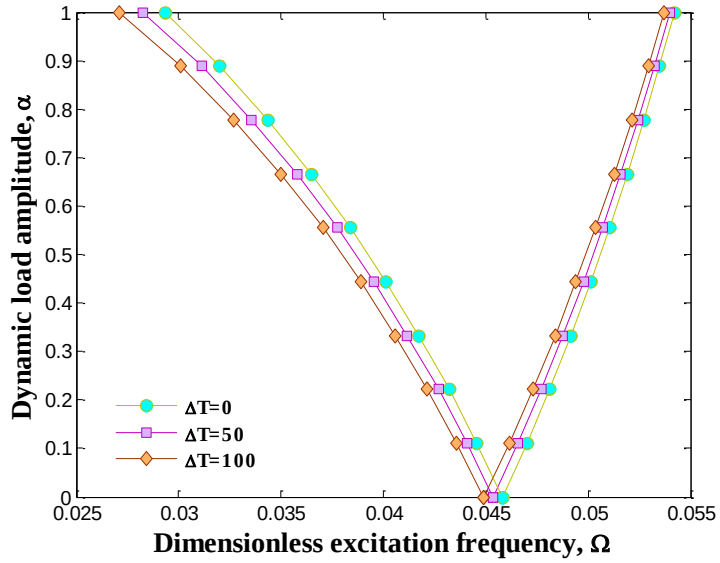

Fig. 11 The effect of temperature gradient on the DIR of structure

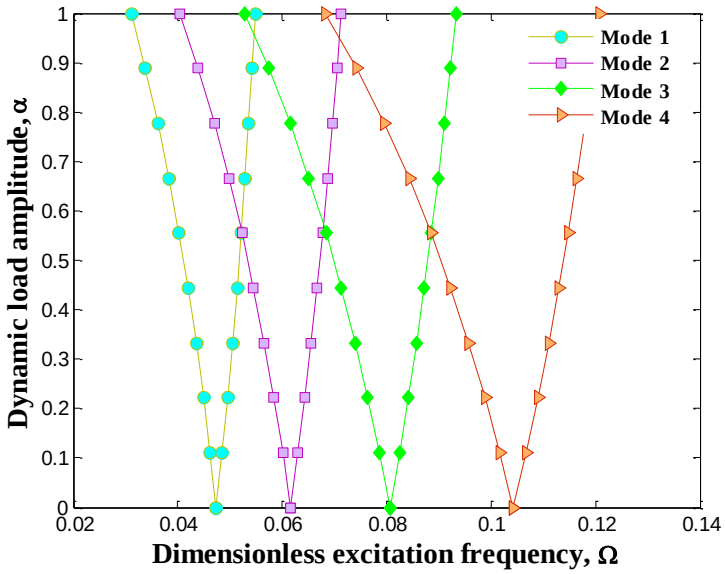

Fig. 12 The effect of mode number on the DIR of structure

Fig. 11 shows the effect of temperature gradient on the DIR of the CNT-reinforced visco-micro-cylindrical shell. As can be seen, increasing the temperature gradient leads to higher resonance frequency and DIR moves to higher frequencies. It is due to the fact that with increasing

the temperature gradient, the structure becomes softer.

The effect of mode number on the DIR of the structure is depicted in Fig. 12. It can be seen that with increasing the mode number, the DIR of the CNT-reinforced visco-micro-cylindrical shell shifts to right and the instability region will be happed at higher excitation frequencies.

6. Conclusions

Dynamic stability analysis of the viscoelastic orthotropic micro cylindrical shell reinforced by FG-CNTs is the main contribution of this work considering the harmonic temperature distribution, 2D magnetic field, orthotropic temperature-dependent properties of the structure in conjunction with the nonhomogeneous orthotropic viscoelastic foundation. After deriving the motion equations by Hamilton's principal, the DQ and Bolotin methods were utilized to calculate the resonance frequency and DIR of structure. The results were found to be in good agreement with the Lei *et al.* (2014). In order to explore the dynamic stability characteristics, the influences of the nonlocal parameter, structural damping, viscoelastic foundation type, boundary condition, mode number, magnetic field, temperature gradient, CNTs volume percent and distribution type on the DIR were also examined. Numerical results indicate that the excitation frequency was significantly influenced by the structural damping. It was found that the FGX-CNT-reinforced visco-micro-cylindrical shell has higher DIR with respect to three other cases. Also, with increasing the CNT volume fraction, the DIR shifts to higher excitation frequencies. In addition, considering size affects and magnetic field leads to higher excitation frequency. Furthermore, increasing the temperature gradient leads to higher resonance frequency. It is hoped that the presented new results can be used as a benchmark solution for future researches.

References

Alibeigloo, A. and Shabanm, M. (2013), "Free vibration analysis of carbon nanotubes by using three-dimensional theory of elasticity", *Acta Mech*., **224**(7), 1415-1427.

Alibeigloo, A. (2014), "Free vibration analysis of functionally graded carbon nanotubereinforced composite cylindrical panel embedded in piezoelectric layers by using theory of elasticity", *Eur. J. Mech. A - Solids*, **44**, 104-115.

Alijani, A., Darvizeh, M., Darvizeh, A. and Ansari, R. (2015), "On nonlinear thermal buckling analysis of cylindrical shells", *Thin Wall. Struct*., **95**, 170-182.

Anon, A. (1996), "FGM components: PM meets the challenge", *Met. Powd. Rep*., **51**, 28-32.

Bich, D.H., VanDung, D., Nam, V.H. and Phuong, N.T. (2013), "Nonlinear static and dynamic buckling analysis of imperfect eccentrically stiffened functionally graded circular cylindrical thin shells under axial compression", *Int. J. Mech. Sci*., **74**, 190-200.

Civalek, Ö. (2016), "Free vibration of carbon nanotubes reinforced (CNTR) and functionally graded shells and plates based on FSDT via discrete singular convolution method", *Compos. Part B*, In press.

Eringen, A.C. (1972), "On nonlocal elasticity", *Int. J. Eng. Sci*., **10**, 1-16.

Esawi, A.M.K. and Farag, M.M. (2007), "Carbon nanotube reinforced composites: Potential and current challenges", *Mater. Des*., **28**(9), 2394-2401.

Fazzolari, F.A. (2015), "Natural frequencies and critical temperatures of functionally graded sandwich plates subjected to uniform and non-uniform temperature distributions", *Compos. Struct*., **121**, 197-210.

Haddadpour, H., Mahmoud khanim, S. and Navazi, H.M. (2007), "Free vibration analysis of functionally graded cylindrical shells including thermal effects", *Thin Wall. Struct*., **45**(6), 591-599.

Hosseini-Hashemi, SH., Abaei, A.R. and Ilkhani, M.R. (2015), "Free vibrations of functionally graded viscoelastic cylindrical panel under various boundary conditions", *Compos. Struct*., **126**, 1-15.
Iijima, S. (1991), "Helical microtubules of graphitic carbon", *Nature*, **354**, 56-58.
Jin, G., Ye, T., Chen, Y., Su, Z. and Yan, Y. (2013), "An exact solution for the free vibration analysis of laminated composite cylindrical shells with general elastic boundary conditions", *Compos. Struct*., **106**, 114-127.
Jin, G., Ye, T., Wang, X. and Miao, X. (2016), "A unified solution for the vibration analysis of FGM doubly-curved shells of revolution with arbitrary boundary conditions", *Compos. Part B: Eng*., **89**, 230-252.
Khalili, S.M.R., Davar, A. and Fard, K.M. (2012), "Free vibration analysis of homogeneous isotropic circular cylindrical shells based on a new three-dimensional refined higher-order theory", *Int. J. Mech. Sci*., **56**(1), 1-25.
Koizumi, M. (1993), "The concept of FGM. ceramic transactions", *Funct. Grad. Mat*., **34**, 3-10.
Kolahchi, R., Hosseini, H. and Esmailpour, M. (2016a), "Differential cubature and quadrature-Bolotin methods for dynamic stability of embedded piezoelectric nanoplates based on visco-nonlocal-piezoelasticity theories", *Compos. Struct*., **157**, 174-186.
Kolahchi, R., Safari, M. and Esmailpour, M. (2016), "Dynamic stability analysis of temperature-dependent functionally graded CNT-reinforced visco-plates resting on orthotropic elastomeric medium", *Compos. Struct*., **150**, 255-265.
Lei, Z.X., Zhang, L.W., Liew, K.M. and Yu, J.L. (2014), "Dynamic stability analysis of carbon nanotube-reinforced functionally graded cylindrical panels using the element-free kp-Ritz method", *Compos. Struct*., **113**, 328-338.
Li, Y.Q. and Tamura, Y. (2005), "Nonlinear dynamic analysis for large-span single-layer reticulated shells subjected to wind loading", *Wind Struct*., **8**(1), 35-48.
Li, S. and Wang, G. (2008), *Introduction to Micromechanics and Nanomechanics*, World Scientific Publication, Singapore.
Liew, K.M., Lei, Z.X. and Zhang, L.W. (2015), "Mechanical analysis of functionally graded carbon nanotube reinforced composites: A review", *Compos. Struct*., **120**, 90-97.
Loy, C.T., Lamm K.Y. and Reddym J.N. (1999), "Vibration of functionally graded cylindrical shells", *Int. J. Mech. Sci*., **41**(3), 309-324.
Madani, H., Hosseini, H. and Shokravi, M. (2016), "Differential cubature method for vibration analysis of embedded FG-CNT-reinforced piezoelectric cylindrical shells subjected to uniform and non-uniform temperature distributions", *Steel Compos. Struct.*, **22**(4), 889-913.
Mirzaei, M. and Kiani, Y. (2016), "Free vibration of functionally graded carbon nanotube reinforced composite cylindrical panels", *Compos. Struct.*, In press.
Mosharrafian. F. and Kolahchi, R. (2016), "Nanotechnology, smartness and orthotropic nonhomogeneous elastic medium effects on buckling of piezoelectric pipes", *Struct. Eng. Mech*., **58**(5), 931-947.
Pradhan, S.C., Loy, C.T., Lam, K.Y. and Reddy, J.N. (2000), "Vibration characteristics of functionally graded cylindrical shells under various boundary conditions", *Appl. Acoust.*, **61**(1), 111-129.
Paliwal, D., Pandey, R.K. and Nath, T. (1996), "Free vibrations of circular cylindrical shell on Winkler and Pasternak foundations", *Int. J. Press. Vessel. Pip*., **69**(1), 79-89.
Pan, Z.W., Dai, Z.R. and Wang, Z.L. (2001), "Nanobelts of semiconducting oxides", *Science*, **291**(5510), 1947-1949.
Qian, D., Wagne,r G.J., Liu, W.K., Yu, M.F. and Ruoff, R.S. (2002), "Mechanics of carbon nanotubes", *Appl. Mech. Rev*., **55**, 495-533.
Rogacheva, N. (1988), "Forced vibrations of apiezoceramic cylindrical shell with longitudinal polarization", *J. Appl. Math. Mech*., **52**(5), 641-646.
Rahimi, G.H., Ansari, R. and Hemmatnezhad, M. (2011), "Vibration of functionally graded cylindrical shells with ring support", *Scient. Iran. B*, **18**(6), 1313-1320.
Reddy, J.N. (2002), *Mechanics of laminated composite plates and shells: Theory and analysis*, 2nd Ed., CRC Press.

Shen, H.S. and Xiang, Y. (2012), "Nonlinear vibration of nanotube-reinforced composite cylindrical shells in thermal environments", *Comput. Method. Appl. M.*, **213-216**, 196-205.
Saito, R., Dresselhaus, G. and Dresselhaus, M.S. (1998), *Physical properties of carbon nanotubes*, Imperial College Press, London.
Song, X., Han, Q. and Zhai, J. (2015a), "Vibration analyses of symmetrically laminated composite cylindrical shells with arbitrary boundaries conditions via Rayleigh-Ritz method", *Compos. Struct.*, **134**, 820-830.
Song, X., Han, Q. and Zhai, J. (2015b), "Vibration analyses of symmetrically laminated compositecylindrical shells with arbitrary boundaries conditions via Rayleigh-Ritz method", *Compos. Struct.*, **124**, 820-830.
Uematsu, Y., Tsujiguchi, N. and Yamada, M. (2001), "Mechanism of ovalling vibrations of cylindrical shells in cross flow", *Wind Struct.*, **4**(2), 85-100.
Wan, H., Delale, F. and Shen, L. (2005), "Effect of CNT length and CNT-matrix interphase in carbon nanotube (CNT) reinforced composites", *Mech. Res. Commun.*, **32**(5), 481-489.
Yakobson, B.I., Brabec C.J. and Bernholc, J. (1996), "Nanomechanics of carbon tubes: Instability beyond linear response", **76**, 2511-2514.
Ye, T., Jin, G. and Su, Z.H. (2016), "Three-dimensional vibration analysis of functionally graded sandwich deep open spherical and cylindrical shells with general restraints", *J. Vib. Control.*, **22**, 3326-3354.
Ye, T. and Jin, G. (2016), "Elasticity solution for vibration of generally laminated beams by a modified Fourier expansion-based sampling surface method", *Comput. Struct.*, **167**, 115-130.
Ye, T., Jin, G. and Su, Z.H. (2016), "A spectral-sampling surface method for the vibration of 2-D laminated curved beams with variable curvatures and general restraints", *Int. J. Mech. Sci.*, **110**, 170-189.
Yu, M.F., Files, B.S., Arepalli, S. and Ruoff, R.S. (2000), "Tensile loading of ropes of single wall carbon nanotubes and their mechanical properties", *Phys. Rev. Lett.*, **84**, 5552-5555.
Zamanian, M., Kolahchi, R. and Rabani Bidgoli, M. (2017), "Agglomeration effects on the buckling behaviour of embedded concrete columns reinforced with SiO2 nano-particles", *Wind Struct.*, **24**(1), 43-57.
Zhou, H., Li, W., Lin, B. and Li, W.L. (2012), "Free vibrations of cylindrical shells with elastic-support boundary conditions", *Appl. Acoust.*, **73**(8), 751-756.

CC